AIP | Review of Scientific Instruments

Low energy, high power hydrogen neutral beam for plasma heating

P. Deichuli, V. Davydenko, A. Ivanov, S. Korepanov, V. Mishagin, A. Smirnov, A. Sorokin, and N. Stupishin

Citation: Review of Scientific Instruments **86**, 113509 (2015); doi: 10.1063/1.4936292
View online: http://dx.doi.org/10.1063/1.4936292
View Table of Contents: http://scitation.aip.org/content/aip/journal/rsi/86/11?ver=pdfcov
Published by the AIP Publishing

Low energy, high power hydrogen neutral beam for plasma heating

P. Deichuli,[1] V. Davydenko,[1] A. Ivanov,[1,a)] S. Korepanov,[2] V. Mishagin,[1] A. Smirnov,[2] A. Sorokin,[1] and N. Stupishin[1]
[1]*Budker Institute of Nuclear Physics, Prospect Lavrentieva 11, 630090 Novosibirsk, Russia*
[2]*Tri Alpha Energy, Inc., Foothill Ranch, California 92610, USA*

(Received 30 July 2015; accepted 10 November 2015; published online 25 November 2015)

A high power, relatively low energy neutral beam injector was developed to upgrade of the neutral beam system of the gas dynamic trap device and C2-U experiment. The ion source of the injector produces a proton beam with the particle energy of 15 keV, current of up to 175 A, and pulse duration of a few milliseconds. The plasma emitter of the ion source is produced by superimposing highly ionized plasma jets from an array of four arc-discharge plasma generators. A multipole magnetic field produced with permanent magnets at the periphery of the plasma box is used to increase the efficiency and improve the uniformity of the plasma emitter. Multi-slit grids with 48% transparency are fabricated from bronze plates, which are spherically shaped to provide geometrical beam focusing. The focal length of the Ion Optical System (IOS) is 3.5 m and the initial beam diameter is 34 cm. The IOS geometry and grid potentials were optimized numerically to ensure accurate beam formation. The measured angular divergences of the beam are ±0.01 rad parallel to the slits and ±0.03 rad in the transverse direction. © *2015 AIP Publishing LLC.* [http://dx.doi.org/10.1063/1.4936292]

I. INTRODUCTION

The neutral beam injection (NBI) has been widely used for plasma heating and sustainment in magnetic fusion devices over the past several decades. NBI has been extensively studied in tokamaks,[1–3] where the ohmic heating alone is insufficient to reach the fusion temperature. Due to the high plasma density and large size of fusion relevant tokamak devices (such as ITER), neutral beams for tokamaks are required to have high energy, from ~0.1 MeV to 1 MeV, high power, e.g., in excess of 33 MW for ITER, and relatively large beam cross section.

As opposed to large tokamaks, in other current plasma confinement devices, such as mirror machines and field reversed configurations (FRCs), relatively low energy and high power neutral beams are required to match the smaller plasma size and weaker magnetic field, which is typical for these experiments.[4–8] To further increase plasma parameters in the gas dynamic trap device[5] and C2-U FRC experiment,[6,7] a novel injector was developed that produces a high power neutral beam at relatively low energy. The injector consists of a plasma source, a beam extractor/accelerator, and a neutralizer. The ion source generates a proton beam with the current of up to 175 A and energy as low as 15 keV. The beam pulse duration is set to 8 ms without active cooling of the grids. The beam extractor/accelerator features multi-slit triode ion optics with spherically shaped grids that provide ballistic beam focusing. Highly accurate ion extraction and focusing allows to achieve a high current density in the neutralized beam, up to ~0.8 eq. A/cm^2 at the focal plane (3.5 m downstream from the grids).

II. ION SOURCE LAYOUT

A. Plasma box

A cutaway view of the ion source is shown in Fig. 1. The diameter and length of stainless steel plasma chamber (2) are equal to 40 cm and 35 cm, respectively. The plasma chamber is surrounded externally by 48 rows of small ceramic Nd–Fe–B magnets (9 mm × 12 mm × 240 mm each) with the alternating magnetization directions, which form a longitudinal line-cusp plasma trap. These magnets are enclosed with the iron yoke. The end plate on the left, which supports four arc-discharge discharge plasma generators (1), is not magnetized. The plasma generators are evenly distributed on a 30-cm-diameter circle. Similar cold cathode arc-discharge plasma generators were used in neutral beam ion sources before, both individually,[9,10] and clustered in a group of two to provide a plasma emitter for high current beam extraction.[11]

The diameter of the discharge channel is equal to 1 cm. In order to increase the plasma output from a plasma generator, a longitudinal magnetic field of 0.1 T is applied to the discharge channel by an electromagnet. The gas (hydrogen) is injected into the discharge channel by gas valves (6) at the cathode and anode. The plasma jets from the plasma generators expand from the 1 cm diameter anode orifices into the cylindrical chamber of the plasma box (2). Since the plasma density in the arc channel is high (~10^{15} cm^{-3}), the hydrogen puffed into the plasma source is almost completely ionized and molecular ions in the plasma are disassociated. During the expansion, the plasma density dramatically decreases. Therefore, additional ionization of the residual gas in the expansion chamber is negligible and the fraction of molecular ion species remains small. As a result, the plasma produced by the arc-discharge plasma sources has a high proton fraction, about 80% or more.

The end of the plasma box opposite to the plasma generators is facing a Cr–Ni bronze plasma electrode of the extractor

a)Electronic mail: ivanov@inp.nsk.su.

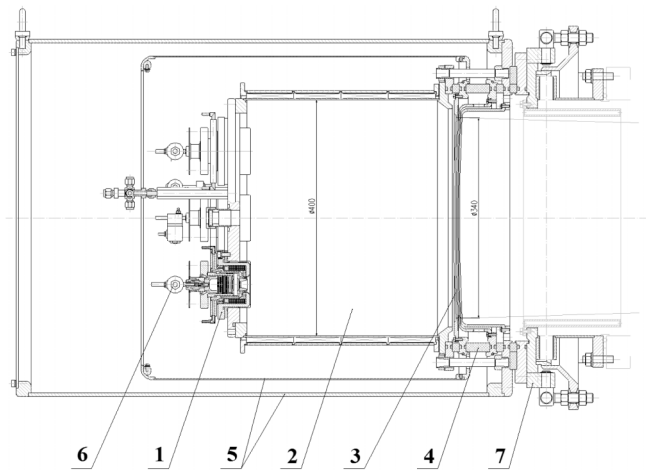

FIG. 1. Injector ion source: 1: arc-discharge plasma generator, 2: expander chamber, 3: grids, 4: insulator, 5: shields, 6: gas valve, 7: aiming gimbal.

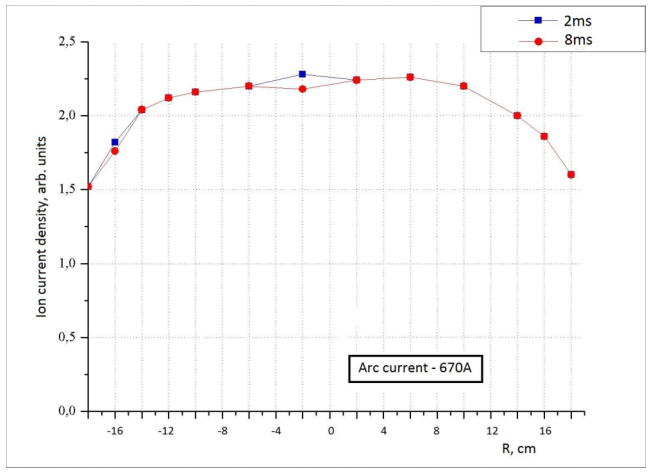

FIG. 2. Ion current density profile at the plasma grid.

(34 cm in diameter) (3), which contains extraction slits each 45 mm long and 2 mm wide. The easy-to-machine Cr–Ni bronze was chosen as a material of the electrode instead of using high melting point metals because the temperature rise of the electrode during the beam pulse was several degrees only.

B. Plasma emitter formation

Typically, a significant part of the plasma generated in the arc-discharges would be lost on the expansion chamber wall, resulting in a plasma flow density decrease. To prevent this loss, the magnets that produce a peripheral multipole magnetic field are installed on the side wall of the plasma chamber. The magnetic field strength at the inner wall of the expander is 0.2 T and decreases to less than 0.01 T at 2 cm radially inwards from the wall. Ion reflection from the peripheral magnetic field increases the plasma flow to the first grid of the ion optical system (IOS) by a factor of 1.5 and provides a more uniform plasma emitter. The plasma flow inside the circle of 340 mm diameter at the first grid emitter reaches 350 A equivalent with the arc current about 1 kA, so that a 175 A ion beam can be extracted. The plasma density near the first grid was measured with a movable triple probe and with a gridded analyzer. The radial profile of the plasma generated by the plasma jets from the arc discharge plasma sources operated each at 670 A of discharge current is shown in Fig. 2. A modulation of the ion current density was observed in the azimuthal direction at the emitter periphery, which is caused by the periodic structure of the magnetic field. To reduce this effect, some optimal gap is necessary between the outer edge of the emitter and the inner diameter of the magnetic wall. As it is seen in Fig. 2, the uniformity of the plasma emitter is high everywhere except for the outer edge where the non-uniformity is about ±15%.

The current density profile at a plane of the plasma grid plane was simulated assuming that the ions in the plasma jets move freely along the straight lines being accelerated in the potential drop next to the anode orifice. Thus, we neglected the electrical fields in the main expansion volume except for the ambipolar electric field generated in the diverging plasma jet near the small cathode orifice due to strong reduction of plasma density in the jet. The spatial distribution of the plasma in the diverging jet is similar to that in the molecular effusion flowfield.[12] In particular, without the magnetic field in the expansion chamber the plasma density upstream of the anode orifice varies as $\cos\theta/r^2$.

The trajectories of the ions, which hit the side wall, were simulated using a calculated profile of the peripheral magnetic

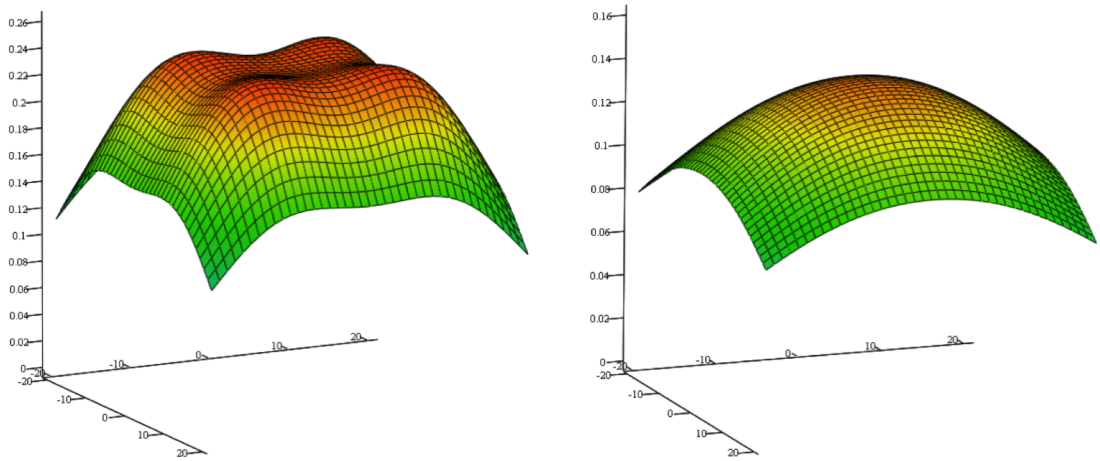

FIG. 3. Simulated profiles of ion current density: 20 cm from the plasma generators (on left) and 35 cm from the plasma generators (on right).

field. A bunch of the ion trajectories originated from the center of anode orifice of each plasma generator was traced to simulate the ion current density profile. The ion pitch angles in the bunch are set by the condition that their angular distribution varies as $\cos\theta \times \sin\theta$. The sampling from this distribution was done by using direct simulation Monte Carlo procedure. This corresponds to the pitch angle setting as $\theta = \arcsin\sqrt{\eta}$ where η is random number uniformly distributed between 0 and 1.[13]

Figure 3 shows the simulated ion current density profile at the distance of 20 cm (left) and 35 cm (right) from the back flange, where the plasma generators are installed. The simulated profiles are found to be in reasonable agreement with the measurements. Absolute value of the ion current density depends upon the plasma density and the electron and ion temperatures.[14]

C. Ion optical system

In the grids, the slots cover an area 340 mm in diameter with 48% transparency. To achieve maximum power density and minimum beam size, the individual beamlets were aimed at a common point 3.5 m from the grids. The ion current of ~150 A is routinely extracted from the plasma emitter and accelerated to an energy of 15 keV. The first grid is in contact with the plasma emitter and has a positive potential of 15 kV. The second grid has negative potential −0.8 kV to create a barrier for electrons of the secondary plasma generated by the beam from the gas bleeding from the ion source and the neutralizer tube. The third grid is grounded. The gas density after the grid was estimated as ~5 mTorr. The grids were formed to be spherical segments with the curvature radius R corresponding to the desirable focal length. The gaps between the plasma and extracting grids slightly vary with radius to compensate for the residual non-homogeneity of the plasma emitter and further optimize formation. The shape of the holes, the gaps, and the grid potentials was optimized for precise beam formation by an electrostatic beam optics computer code PBGUNS.[15] The simulated ion trajectories in the elementary cell of the ion optical system are shown in Fig. 4. These calculations also confirmed that the required barrier for electrons arises at negative potential of −0.8 kV at the second grid.

III. EXPERIMENTAL RESULTS

Tests were carried out at the pulse duration of 8 ms. The accelerating voltage and beam current oscilloscope traces are shown in Fig. 5. The voltage exhibits some periodical variations due to switching of the voltage boosts in the power supply. The beam current, which is determined by the plasma flow

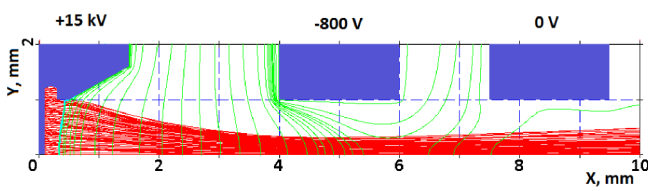

FIG. 4. Simulated trajectories in the elementary cell of the ion optical system.

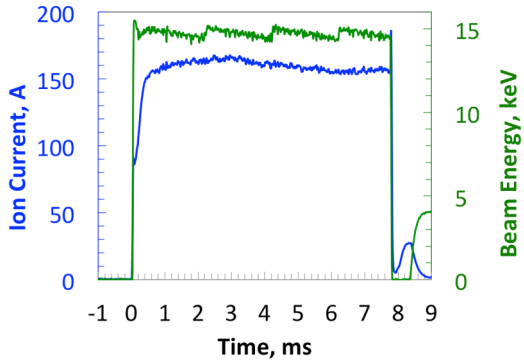

FIG. 5. Extracted beam current and voltage.

from the arc-discharge plasma generators, does not respond to these variations. Beam radial profiles are measured at several axial locations along the beamline with secondary electron emission detectors and with a retractable calorimeter. The scan of the beam width versus the beam current at 4 m from the source is shown in Fig. 6. It displays the typical V-shape dependence with a minimum beam size corresponding to the optimal perveance at the ion current of ~160 A. The beam profile measurements at two distances from the source (3.5 and 4 m) allow to estimate the focal length, which is found to be 350 ± 25 cm at the grid curvature of 350 cm, in a good agreement with the calculated focus length. Also inferred from the profile measurements are the beam divergence half-angles across and along the slits, 0.03 and 0.01 rad, respectively. In the simulations,[16] the minimal beam divergence across the slit was found to be ~0.025 rad and 0.01 rad along the slit in a reasonable agreement with the experimental data.

The equivalent current density exceeding 0.8 eq. A/cm^2 was achieved at the beam focal plane.

The beam species were measured with an optical spectrometer. The measured Doppler-shifted spectrum of the beam radiation is shown in Fig. 7. The energy fractions analysis based on a model described in Refs. 17 and 18 indicates that H^+, H^+_2, and H^+_3 percentages in the extracted beam (at 160 A) are 85%, 10%, and 4%, respectively. The water is initially low (~1%) and gradually conditions away.

Similar results for the beam composition were obtained with the measurements of the beam species with magnetic mass-spectrometer measurements.

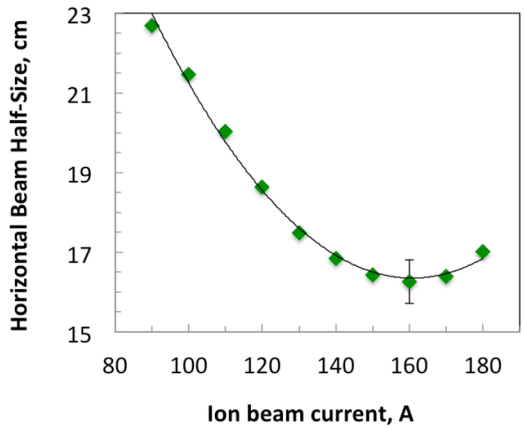

FIG. 6. Horizontal beam half-width measured at 4 m from the grids.

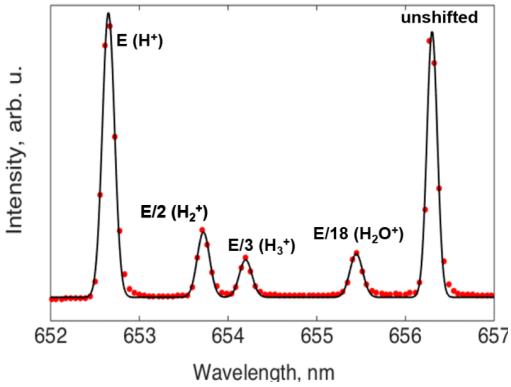

FIG. 7. Doppler-shifted beam emission.

IV. CONCLUSIONS

A high power hydrogen beam injector was developed and tested at the beam energy of 15 keV and the ion beam current of up to 175 A. The arc-discharge plasma emitter provides about 85% of H^+ in the ion current. The distinguishing feature of the injector is the capability of strong beam focusing, so that after neutralization in a gas target, the high power beam can be transmitted through a narrow port to plasma.

ACKNOWLEDGMENTS

The authors would like to acknowledge Dr. T. Akhmetov for his assistance with the beam profile data analysis. This work was supported by the Russian Science Foundation (Project No. 14-50-00080).

[1]G. G. Kelley, O. B. Morgan, L. B. Stewart, W. L. Stirling, and H. K. Forsen, Nucl. Fusion **12**, 169 (1972).
[2]L. A. Berry, J. D. Callen, R. J. Colchin, G. G. Kelley, J. F. Lyon, and J. A. Rome, Phys. Rev. Lett. **34**, 1085 (1975).
[3]M. M. Menon, Proc. IEEE **69**, 1012–1029 (1981).
[4]A. W. Molvik, R. H. Munger, T. J. Duffy, and D. L. Correll, Rev. Sci. Instrum. **52**(7), 965 (1981).
[5]P. A. Bagryansky, A. G. Shalashov, E. D. Gospodchikov *et al.*, Phys. Rev. Lett. **114**, 205001 (2015).
[6]M. Tuszewski *et al.*, Phys. Rev. Lett. **108**, 255008 (2012).
[7]M. W. Binderbauer *et al.*, Phys. Plasmas **22**, 056110 (2015).
[8]J. Waksman, J. K. Anderson, M. D. Nornberg *et al.*, Phys. Plasmas **19**, 122505 (2012).
[9]P. P. Deichuli, V. I. Davydenko, S. A. Korepanov *et al.*, Rev. Sci. Instrum. **75**, 1816 (2004).
[10]V. I. Davydenko and A. A. Ivanov, Rev. Sci. Instrum. **75**, 1809 (2004).
[11]J. K. Anderson, A. F. Almagri, B. E. Chapman *et al.*, Trans. Fusion Sci. Technol. **59**, 27 (2011).
[12]G. A. Bird, *Molecular Gas Dynamics and the Direct Simulation of Gas Flows* (Clarendon Press, Oxford University Press, New York, 1994), p. 153.
[13]G. A. Bird, *Molecular Gas Dynamics and the Direct Simulation of Gas Flows* (Clarendon Press, Oxford University Press, New York, 1994), p. 423.
[14]I. A. Kotel'nikov and V. T. Astrelin, Phys.-Usp. **58**(7), 701 (2015) (in Russian).
[15]J. E. Boers, J. Vac. Sci. Technol. **10**, 1120 (1973).
[16]V. Davydenko *et al.*, Rev. Sci. Instrum. **87**, 02b303 (2016).
[17]R. Uhlemann, R. S. Hemsworth, G. Wang, and H. Euringer, Rev. Sci. Instrum. **64**, 974 (1993).
[18]S. V. Polosatkin, A. A. Ivanov, A. A. Listopad, and I. V. Shikhovtsev, Rev. Sci. Instrum. **85**, 02A707 (2014).